J. Membrane Biol. 70, 115–123 (1982)

The Journal of
Membrane Biology

Periaxonal Surface Calcium Binding and Distribution of Charge on the Faces of Squid Axon Potassium Channel Molecules

Jurgen F. Fohlmeister* and William J. Adelman, Jr.**
Laboratory of Biophysics, Marine Biological Laboratory, Woods Hole, Massachusetts 02543

Summary. The calcium binding constant associated with external surface charge in a position to influence the voltage sensing charges for potassium channel gating appears to be $\sim 30\,\text{molar}^{-1}$, a value much larger than previously thought and in approximate agreement with that found for artificial membranes composed of the lipid brain phosphatidylserene. Fixed charge on the periaxonal membrane surface is distributed in such a way that much larger charges occur at a distance of at least 8 angstroms from the channel pore openings. The separation between the ion pathway and the channel gating charge appears to be greater than or equal to 8 angstroms. Periaxonal surface charge which is in a position to determine the surface potential for gating has a magnitude greater than or equal to one (negative) electronic charge per 182 square angstrom before calcium binding, which is reduced to $-e/625\,\text{Å}^2$ in a normal divalent ionic environment. With the normal divalent ionic composition of seawater the surface potential at a position to influence the gating voltage sensor is ~ -15 millivolts relative to the bulk external potential. The external surface potential is ~ -3 mV at the pore mouth. There appears to be a negligible amount of fixed charge on the axoplasmic surface in the vicinity of the ion channel opening. Further, our results confirm earlier measurements that have given a negligible amount of axoplasmic surface fixed charge whose field components would be in a position to influence the channel gating charges.

Key Words surface charge · calcium binding · potassium channel · axon membrane · surface potential

Introduction

Electric charges associated with polar groups at the surface of biological membranes produce components of the electric field within the membrane and therefore can act on such biophysical factors as the local ionic driving force within excitable channels and channel gating (Frankenhaeuser & Hodgkin, 1957; Gilbert & Ehrenstein, 1969). That the charge is not uniformly distributed on the membrane surface follows from the observation that manipulations intended to alter its value produce different apparent membrane potential shifts in the sodium and potassium channel gating kinetics (Chandler, Hodgkin & Meves, 1965). Calculations using the "diffuse double-layer theory" (Grahame, 1947) further indicate that the charge density on lipid bilayers composed of brain phosphatidylserine – a major constituent of the squid axon membrane – is much larger than charges associated with ion channel molecules (McLaughlin et al., 1981). Because of the special significance of electrical properties to electrically excitable channels we attempt a degree of spatial resolution of the surface charge associated with one of these (the K channel) using the voltage-clamp technique.

For this purpose it is necessary to identify at least two factors that contribute to the ionic conductance and whose physical mechanisms are separated spatially in the plane of the membrane. Otherwise the same surface charge will influence the several factors equally and the charge density will not be spatially resolved. Two obvious factors for excitable channels are 1) that they are gated (with individual channels being either open or closed; Conti & Neher, 1980; Sigworth & Neher, 1980), and 2) that the population of open channels constitutes some sort of passive diffusion regime (which appears to be single-file diffusion in individual channels; e.g., Hodgkin & Keynes, 1955; Hille & Schwarz, 1978). The first indication that the mechanisms of these two aspects may be spatially separate came from a study of the saxitoxin binding properties to sodium channels (Henderson, Ritchie & Strichartz, 1973). The gating for that channel consists of at least the two components of activation and inactivation, and if these do not

* *Permanent address:* Department of Physiology, University of Minnesota, Minneapolis, Minn. 55455.
** *Permanent address:* Laboratory of Biophysics, Intramural Research Program, NINCDS, National Institutes of Health at the Marine Biological Laboratory, Woods Hole, Mass. 02543.

0022-2631/82/0070-0115 $01.80

Table 1.

Internal Solutions Compound	150	300	450 mM K^+
KF	25	50	75
K glutamate	100	200	300
K_2HPO_4	12.5	25	37.5
Sucrose	792.5	505	217.5
Ionic strength	288	575	863
Osmolarity	1041	1009	968

External Solutions K^+	Ca^{++}	Na^+	Cl^-	Osm
50	2	467	521	879
	10	455	525	872
	40	410	540	869
	100	320	570	882
10	2	507	521	879
	10	495	525	872
	40	450	540	869
	100	360	570	882

Above quantities are millimolar.
TTX = 0.2 μM; Tris = 20 mM; pH = 7.4.

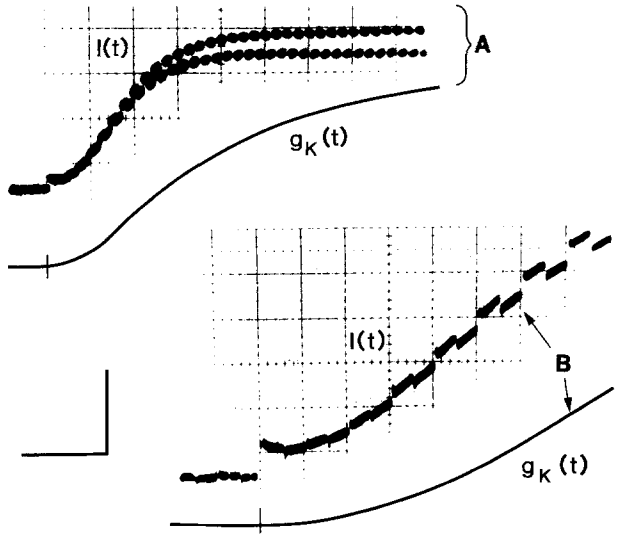

Fig. 1. Time course of membrane current for a "ric-rac" depolarization to +30 mV from a holding potential of −60 mV at 4.5 °C, and derived instantaneous K^+ conductances. $[Ca^{++}]_e = 40$ mM, $[K^+]_e = 10$ mM and $[K^+]_i = 300$ mM. Ordinate bar is 1.25 mA/cm² and 40.0 mmho/cm² for curves *A* and 0.5 mA/cm² and 16.0 mmho/cm² for curves *B*. Abscissa bar is 4 msec for *A* and 1 msec for *B*. $g_K = 0.5$ mmho/cm² under the conditions just prior to the main clamp step

share a common electric field probe (*cf.* Moore & Cox, 1976; Schauf, 1976; Jakobsson, 1978) a further degree of resolution of the surface charge density may be possible there.

In this paper, the relative surface potential shifts which influence each of the two components (the pore and the gate) of the potassium channel are measured at the internal surface for a series of solutions of decreasing ionic strength. At the external membrane surface, the relative surface potentials are measured for a series of calcium concentrations in the external solution. A theory of the "diffuse double layer" in conjunction with specific calcium binding to negative polar groups (Mozhayeva & Naumov, 1970; McLaughlin, Szabo & Eisenman, 1971) is then used to calculate values of the absolute surface potentials, the fixed surface charge densities and a calcium association constant. A self-consistent picture emerges which suggests that the channel molecule is relatively neutral electrically on its surfaces, and that a charged group with a relatively high binding affinity for calcium exists on the periaxonal surface at some distance from the pore.

Material and Methods

Voltage-Clamp Techniques

Giant axons from the hindmost stellar nerve of the squid *Loligo pealei* were internally perfused and voltage-clamped using double pulse and "ric-rac" pulse (Adelman, 1979) techniques. Experiments were carried out at two temperatures, 4.6 ± 0.3 °C and 9.0 ± 0.2 °C.

Internal solutions were Na^+-free and are listed in Table 1. The solutions were chosen to obtain a range of internal ionic strengths (Chandler et al., 1965). Sodium ions were excluded because of their blocking action on K channels (French & Wells, 1977). pH was adjusted to 7.2 with free glutamic acid.

External solutions were Mg^{++}-free and are listed in Table 1. 0.2 μM TTX blocked the Na-channels completely. Experiments were performed with eight different combinations of external Ca^{++}- and K^+-concentrations ($[Ca^{++}]_e = 2$, 10, 40 and 100 mM and $[K^+]_e = 10$ and 50 mM) with Na-ions used in place of calcium and potassium to maintain a total external ionic strength of ~1080 mM.

The clamp was compensated for a series resistance of 2 Ω cm² as in Binstock, Adelman, Senft and Lecar (1975). This value was measured for intact axons of 500 μm diameter for which approximately half of the resistance is due to the axoplasm. Since the specific resistance of the high internal ionic strength solution (863 mM) is in the range of 22 to 25 Ω cm, and of the low ionic strength solution (288 mM) in the the range of 60 to 65 Ω cm, as compared with that of axoplasm (37 to 41 Ω cm, *cf.* Binstock et al., 1975), the actual series resistance may have varied from 1.6 to 2.4 Ω cm². Therefore, for the maximum membrane conductance of ~90 mmho/cm² measured herein, the maximum error in membrane potential introduced by this variation in actual series resistance is estimated to be ±3%. This percentage error decreases almost proportionately with the magnitude of membrane conductance.

The voltage pulses used in the double-pulse technique consisted of test depolarizations in the range of −20 to +105 mV from a holding potential of −60 mV. Measured junction potentials were compensated. At various times (in the range of $t = 0.5$ to 30 msec) following the onset of the test pulse, the potential was abruptly incremented by 10 mV and clamped for 1 msec before returning to the holding potential where it was held

for 9 sec. Instantaneous conductance was calculated from the measured current difference (corrected for leakage current) divided by the voltage increment (*see below*).

The "ric-rac" pulse technique was used to supplement the data from the two pulse experiments. Ric-rac voltages consisted of a train of 5 mV peak-to-peak, 2000/sec square waves centered on the test voltage pulses listed above. Figure 1 shows sample records along with the time courses of the derived instantaneous conductance. Justification of the ric-rac amplitude and frequency is given in Fohlmeister and Adelman (1982).

Separation of Gating and Ionic Driving Force

In order to determine the surface potentials near the opening of the pore, we analyze the ionic driving force uncontaminated by gating processes. For this analysis we make the assumption that the K current can be written as the product

$$I_K = \hat{g}_K \cdot P_K \cdot f(E), \tag{1}$$

where $\hat{g}_K$ is a constant with the units of conductance, $f(E)$ is a voltage-dependent function that is *independent* of electrical gating, and P_K is the portion that varies in accordance with electric field gating. In view of the recent finding that a single K-channel is either open or closed without intermediate conductance states (Conti & Neher, 1980), P_K is defined as the probability that a randomly chosen single channel is in the open state (*cf.* Fohlmeister & Adelman, 1981). We assume further in accordance with the properties of *delayed* rectification that P_K will not change stepwise in response to a voltage-clamp step in E. Instantaneous conductance $g_K(t)$ can then be measured with a small voltage increment ΔE at time t, and is defined by

$$g_K \equiv \frac{I_K^+ - I_K^-}{\Delta E} = \hat{g}_K \cdot P_K \cdot \frac{f(E^+) - f(E^-)}{\Delta E}$$

$$\xrightarrow{\Delta E \to 0} \hat{g}_K \cdot P_K \cdot \frac{df}{dE} \tag{2}$$

where I_K^+ is the K-current immediately following, and I_K^- is the K current immediately preceding the voltage step ΔE from E^- to E^+. (To be strictly correct, df/dE may be written as a partial derivative $\partial f/\partial E$, because f can depend on ion activities in addition to the membrane potential E.) By dividing the potassium currents I_K^- by the instantaneous conductances we arrive at the "instantaneous driving force"

$$A(E) \equiv \frac{I_K}{g_K} = f / \frac{dF}{dE} \tag{3}$$

from which $f(E)$ is derived to within a multiplicative constant. All factors that depend on voltage gating are cancelled in this expression. Both I_K and g_K are directly measured quantities. As their ratio, $A(E)$ equals the slope of the straight line drawn through data points of I_K plotted against g_K measured at various times during the rising phase of these variables under voltage-clamp (e.g., Fig. 4 and 5). For measurements concerning the instantaneous driving force A, which depends on the activities of the conducting ions in general, instantaneous conductance was measured during the first 3 to 4 msec following the onset of depolarization. This minimizes possible problems of data interpretation due to the accumulation of K^+ in the periaxonal space.

As the potential of depolarizing voltage-clamp is increased, the steady-state potassium conductance increases for moderate depolarizations and then "bends over" towards an upper limit plateau for large depolarizations (e.g. Figs. 2 and 3). We use this nonlinear property of g_K vs. E to determine the relative voltage shift brought about by changes in surface potential which is in a position to influence the electric field strength at the "voltage sensor" for the channel gate.

Surface Charge, Surface Potential and Calcium Binding

Surface potentials Ψ_s and associated surface charge densities σ are calculated from the Grahame equation (Grahame, 1947)

$$\sigma^2 = \frac{kT\varepsilon}{2\pi} \sum_i C_i [\exp(-z_i e \Psi_s / kT) - 1] \tag{4}$$

where C_i is the bulk ion concentration of the i'th species in moles per liter, z_i is its valence, Ψ_s is the electrostatic potential relative to the bulk potential, $kT/e = 23.8$ mV at 4.6 °C, and $kT\varepsilon/2\pi = 1.20 \times 10^{-5}$ in an aqueous solution to yield a surface charge density σ, in units of electronic charges per square angstrom.

We find that this equation is inadequate to describe the electrostatic surface effects and therefore generalize the theory to include specific calcium binding to charged surface groups:

$$\sigma = \sigma_0 / [1 + K \cdot C_{Ca} \cdot \exp(-2e\Psi_s / kT)]. \tag{5}$$

In this equation σ_o is the surface charge density in the absence of calcium, K is the calcium association constant in $(\text{moles})^{-1}$ (McLaughlin et al., 1971) and the Boltzmann factor, $\exp(-2e\Psi_s/kT)$, is included as a measure of the local enhancement of calcium concentration due to the *final* surface charge σ. Specific surface adsorption of monovalent cations is not considered herein since we find no evidence for its existence on the K-channel molecule (*cf.* Eisenberg, Gresalfi, Riccio & McLaughlin, 1979).

Results

Fixed Charge and the Electric Field Probe for the Gate

Periaxonal Surface. Instantaneous conductance (g_K) was measured in the steady-state phase of voltage-clamp pulses (E) for a series of external calcium concentrations ([Ca] = 2, 10, 40 and 100 mM) and for a series of test potentials. These data are plotted in Fig. 2 (g_K versus E). Each curve reaches a plateau for the larger test potentials. The membrane potentials $E_{1/2}$ for which the instantaneous conductances are precisely half of the plateau values are listed in the inset of Fig. 2. The shifts in the $E_{1/2}$ values with $[Ca]_e$ are attributed to changes in the electric field at the gating voltage sensor, fields that are altered in response to a shifting surface potential.

Further analysis shows that the curves of Fig. 2 superimpose when their plateau values are normalized and the curves are shifted by a characteristic amount along the voltage axis. For this procedure the characteristic voltage shifts are −10 mV for [Ca] = 10 mM, −17 mV for 40 mM and −22 mV for 100 mM calcium relative to the voltage for 2 mM

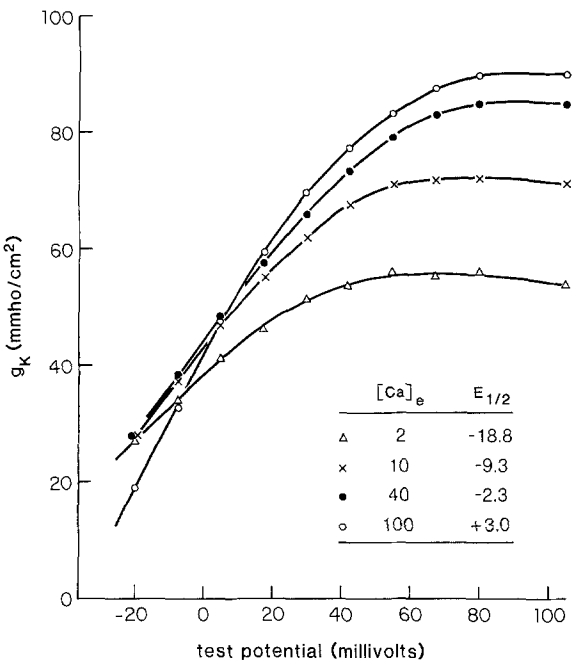

Fig. 2. Instantaneous conductances g_K measured in the steady-state phase of voltage-clamp pulses plotted against the test potential for a series of [Ca] (*see* curve labels) and for $[K]_i/[K]_e =$ 300 mM/10 mM. Data from one typical axon

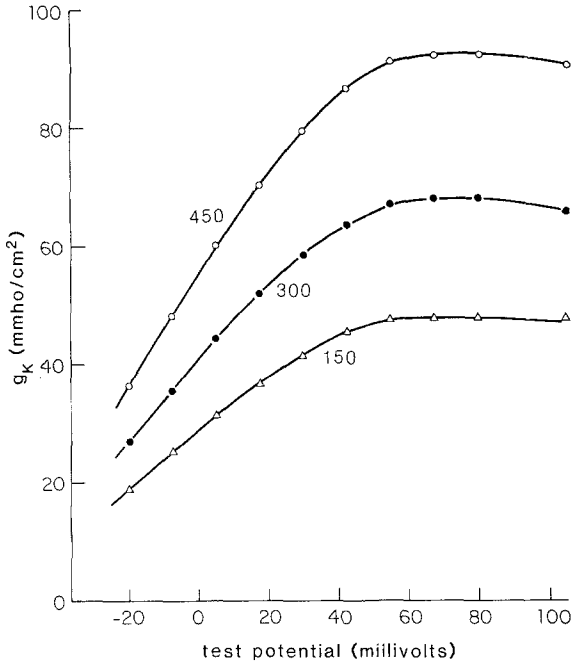

Fig. 3. Instantaneous conductances g_K measured in the steady-state phase plotted against test potential for a series of internal K concentrations (*see* curve labels). Data from one typical axon

Table 2. Shifts for individual axons along the voltage axis of the "universal" g_K vs. E curve for 10, 40 and 100 mM [Ca] relative to 2 mM [Ca][a]

Axon	10 (mV)	40 (mV)	100 mM Ca (mV)
A-6	−9.6	−16.5	−21.4
A-8	−9.9	−16.9	−21.8
A-9	−10.4	−17.5	−22.5
A-13	−10.6	−17.7	−22.4
A-14	−10.2	−16.9	−21.8
A-16	−9.0	−15.9	−21.0
A-17	−10.1	−17.0	−21.5
A-20	−10.2	−18.0	−22.9

[a] The quantitative pattern remained for seven further axons for which partial data were obtained

Table 3. Residual surface charge density and absolute surface potential as functions of [Ca]

Surface Charges and Potentials		
[Ca]	σ [$-e$/Å²]	Ψ_s [mV]
100	0.00086±0.0003	− 7±2
40	0.0013 ±0.0004	−12±2
10	0.0022 ±0.0004	−19±2
2	0.0033 ±0.0004	−29±2

$\sigma_o = -e/182$ Å; $K = 30$ M^{-1}.

[Ca]. A curve segment shifted by an incorrect amount will not fall on the "universal" g_K vs. E curve. Since g_K varied slightly among axons, the fitting procedure was done for data on each axon separately. Shifts for individual axons are listed in Table 2.

Surface charge density and absolute surface potentials were calculated from Eqs. (4) and (5). The fitting procedure began with the simplest, and most restrictive assumption [namely the possible adequacy of the theory as expressed by Eq. (4) alone] and was then generalized to include the effects of calcium binding [Eq. (5)] when the simpler assumption was found inadequate (*see* Discussion and Fig. 6). Each of the general expressions (4) and (5) becomes a set of four equations – one for each combination of ionic concentrations used in the four external solutions. The criterion used to judge a theory as adequate (i.e. sufficient) was that the number of variables to be determined be smaller than the number of independent equations comprising the theory, and that a set of values of the variables could be found that simultaneously satisfied all of the equations whose coefficients are based on the data. When calcium binding is disregarded the two variables to be determined are σ and the one free parameter that fixes the absolute level of the measured relative potentials [a free parameter that corresponds to parameter B of Gilbert and Ehrenstein, 1969, Eq. 11)]. No set of values of these two variables fit all four equations simul-

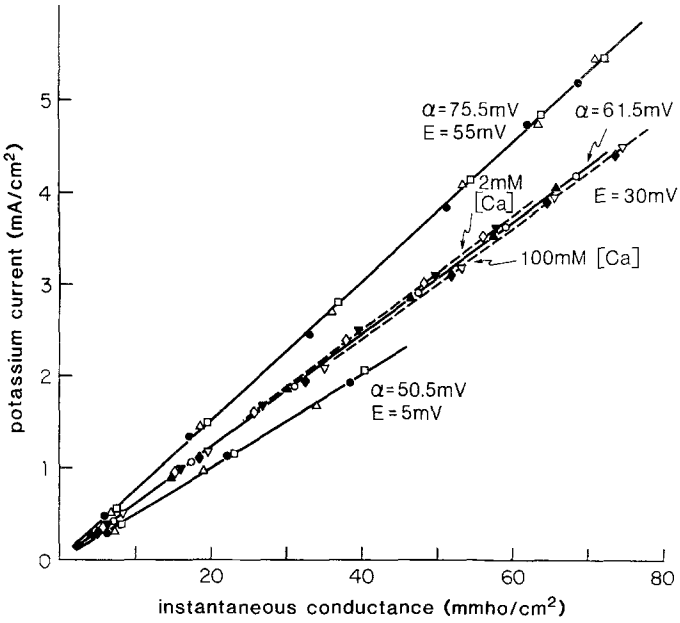

Fig. 4. Potassium current (I_K^- in text) plotted against instantaneous K conductance g_K for 5 combinations of test potentials and calcium concentrations. Solid lines connect data points obtained for [Ca]=10 mM and $E+55$ (●, △, □) upper, $+30$ (▲, ○) middle, and $+5$ mV (●, △, □) lower. Dashed lines connect data points obtained for [Ca]=2 mM (◇, ▼) and 100 mM (◆, ▽) and for $E=30$ mV. Data points correspond to 0.5, 1, 1.5, 2, 2.5 and 3 msec (for $E=55$ and 30 mV), and to 1, 2 and 3 msec (for $E=5$ mV) following the onset of the voltage-clamp pulse. Data are from 3 representative axons

taneously. However, with calcium binding included a set of values for the seven variables (the set of four σ's, σ_o, K and the parameter that fixes the absolute surface potential) could be found that simultaneously satisfied the set of eight Eqs. (4) and (5). A method of successive approximation was used to achieve a best fit of $\sigma_o = -e/182$ Å^2 and $K=30$ M^{-1}. The experimental error in the measured relative surface potentials brackets the variables to $-e/195$ Å$^2 \leqq \sigma_0 \leqq -e/150$ Å^2 and $14 \leqq K \leqq 60$ M^{-1}. Values of absolute surface potentials Ψ_s and surface charges σ are listed in Table 3 for the set of experimental calcium concentrations.

Axoplasmic Surface. The procedure of determining $E_{1/2}$ values and of fitting experimental conductance versus voltage (g_K vs. E) curves was repeated for a series of internal K ion concentrations ($[K^+]_i$=450, 300 and 150 mM). These represent a series of total internal ionic strength (*see* Table 1). Differences in internal surface charge screening by different ionic strengths should lead to a voltage shift among the curves as predicted by the Grahame equation. No shift is observed in the data (Fig. 3). We conclude therefore that there is a negligible amount of surface charge on the internal membrane surface, at least not in a position to influence the "electric field probe" of the potassium channel gates.

Fixed Charge at the Mouths of the Pore

Periaxonal Surface. The driving force $A(E)$, which is defined in Eq. (3), was measured for a calcium series of external solutions, each for a set of test potentials E. A was found to be a relatively strong function of the test potential, but a weak function of $[Ca]_e$ (Fig. 4). Internal and external K concentrations were held constant for this test ($[K^+]_i$= 300 mM, $[K^+]_e$=10 mM) as was the ionic strength with Na ions used as a replacement for calcium

This test was repeated using other K-concentrations ($[K^+]_i/[K^+]_e$=450/5, 300/50 and 150/50, all millimolar) with similar results. Since the chemical potential gradient across the membrane was held constant during each test, the relatively small effect with changes in $[Ca^{++}]_e$ indicates that the electric field across the membrane remains relatively unchanged. From this, we conclude that the surface potential at a position to influence the driving force – namely near the external pore mouth – is relatively small. Comparing changes in $A(E)$ for [Ca] variations with those for test potential changes we conclude that the external surface potential decreases (becomes more negative) by ~4 mV in going from 100 to 2 mM calcium (Fig. 4). Analysis shows further that the magnitude of the surface potential near the external pore opening is ~5 mV negative for [Ca]=2 mM (*see* Discussion).

Axoplasmic Surface. To determine the potential near the pore mouth at the internal membrane surface, $A(E)$ was measured for a series of internal K concentrations ($[K^+]_i$=450, 300 and 150 mM) and for a range of test potentials. Total internal ionic strength varied as before from approximately 288 to 863 mM (for 150 to 450 mM K^+, respectively). The measured $A(E)$ showed the usual strong

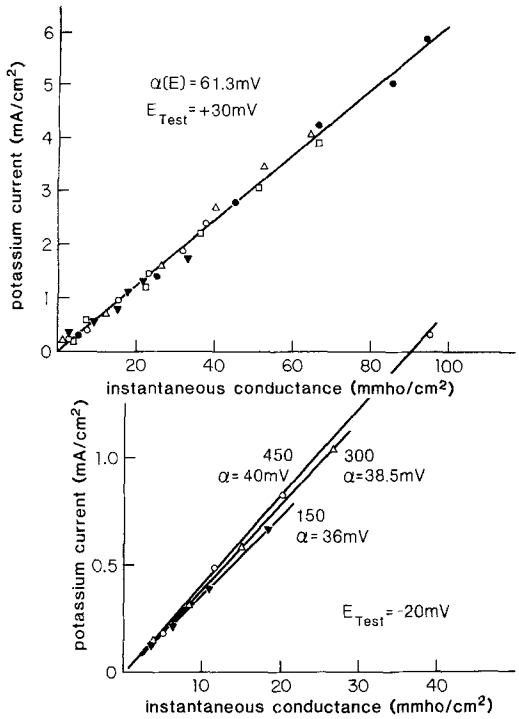

Fig. 5. Potassium current (I_K^- in text) plotted against instantaneous conductance. [Ca]=10 mM for all plots. *Upper Panel*: Three internal K-concentrations were used [150 (▼, ○), 300 (△, □) and 450 (●) mM for measured total ionic strengths of 288, 575 and 863 mM, respectively] in conjunction with two external K-concentrations [10 (●, □, ▼) and 50 (△, ○) mM]. Data points correspond to 0.5, 1, 1.5, 2, 2.5 and 3 msec following the onset of the voltage-clamp pulse to $E=30$ mV. Data points are samples from 15 axons (2 from each axon "randomly" selected to show the degree of reproducibility). *Lower Panel*: Slopes (values of A) for three internal ionic strengths and a test potential of $E=-20$ mV. Lines are labeled with the internal K-concentrations (in mM). External K-concentration was 10 mM. Data points correspond to 1, 2, 3 and 4 msec following the onset of the voltage clamp pulse and are from one representative axon.

dependence on test potential E, but was entirely independent of changes of internal ionic strength (changes in $[K^+]_i$) for $E=+55$ and $+30$ mV (Fig. 5, upper panel). The experimental error allows this determination to within ± 2 mV. If there is any fixed charge in a position to influence the surface potential, diffuse double-layer theory predicts a shift in surface potential with a shift in ionic strength (Grahame, 1947; Fohlmeister & Adelman, 1982). We therefore interpret the *absence* of a potential shift to imply the *absence* of surface charge near the internal surface pore mouth.

The measured driving force $A(E)$ began to show some systematic variation with ionic strength for the smaller depolarizations of $E=+5$ and -20 mV (*see* Fig. 5, lower panel). These variations for the smaller depolarizations have an explanation consistent with the absence of surface charge (*see* Discussion).

Discussion

Surface Charge, Potentials, and Gating Kinetics

Periaxonal Surface Charge and Channel Gating. Apparent membrane voltage shifts that influence the potassium conductance of the squid axon were measured by Frankenhaeuser and Hodgkin (1957), and showed an increase of 10–15 mV for a fivefold reduction in $[Ca^{++}]_e$. No measurements of surface charge (whose possible existence was suggested by A.F. Huxley) or absolute surface potential were attempted by them. Gilbert and Ehrenstein (1969) working with the squid axon in high external potassium concentrations calculated $\sigma_o = -e/120$ Å^2 (with a minimum of $-e/280$ Å^2) with a calcium association constant $K=0.1$ M^{-1}. Begenisich (1975), working with intact *Myxicola* giant axons, measured an apparent voltage increase of 6 mV for a fivefold reduction in $[Ca^{++}]_e$ and calculated a surface charge density of $-e/275$ Å^2 to $-e/350$ Å^2 with a calcium association constant $K=0$ to 0.2 M^{-1}.

Our data give a best agreement with Eqs. (4) and (5) for $\sigma_0 = -e/180$ Å^2 with a calcium association constant of ~ 30 M^{-1}. This conclusion was reached by assuming various sets of absolute surface potentials Ψ_s spaced by the measured relative values for the experimental $[Ca^{++}]$ series and computing the resultant series of surface charge densities. The curve pairs in Fig. 6 show the best possible overlap between net surface charges σ computed from Eq. (4) and (5) separately. For a given set of absolute surface potentials the curves as calculated from Eq. (4) (●) are then fixed. For a given value of K in Eq. (5) (○), changing the value of σ_o shifts its curve up or down by a constant factor. The difference in the *shapes* within each pair of curves for small $K(=0.1$ M$^{-1})$ cannot be reconciled without assuming arbitrary errors in the measured relative surface potential shifts. Since we consider this unlikely, we conclude that K is in the range of 14 to 60 M^{-1}. For the best fit of $K=30$ M^{-1} half of the surface charge is neutralized by bound calcium when the calcium concentration is ~ 33 mM at the position of the compact double layer (i.e. the membrane surface).

To bring a curve pair into coincidence to the degree shown in Fig. 6*B*, note that the value of K increases significantly (from 0.1 to 30 M^{-1}) with an accompanying decrease in the absolute surface

potential from $\psi_{ASW} = -58$ to -15 mV (Fig. 6*A*). This property is the clue to reconciling the earlier results with our conclusions.

The data of Gilbert and Ehrenstein (1969) are fit equally well by taking parameter B [their Eq. (11)] to equal -25 to -30 mV. This reduces the magnitude of their calculated external surface potential from ~ -60 to ~ -30 mV for a divalent cation concentration equal to that in normal sea water, and implies a calcium association constant $K \approx 30\ \text{M}^{-1}$ and $\sigma_0 \approx -e/180\ \text{Å}^2$.

Similarly, the data of Begenisich (1975) can be fit with $K = 60$ to $150\ \text{M}^{-1}$ and $\sigma_0 = -e/490\ \text{Å}^2$ to $-e/360\ \text{Å}^2$, respectively, with a surface potential of ~ -6 mV in sea water with normal divalent cation concentrations (Fig. 6*C*, lowest curve).

Although there is some discrepancy between these two sets of values of K, σ_0 and Ψ_s (determined under different conditions and for different preparations), they both imply a much larger calcium association constant and somewhat smaller surface charge density and absolute surface potential than was previously considered. In particular, the determination of the association constant did not include saturation effects of calcium binding. Indeed, by assuming very small association constants ($K \sim 0.1\ \text{M}^{-1}$), one cannot expect to see saturation effects at the experimental calcium concentrations ([Ca] $\leqq$ 160 mM). However, the data of Begenisich (1975, Table III) do in fact suggest the beginning of saturation for calcium concentrations of 100 mM. The data of Gilbert and Ehrenstein (1969) suggest a similar saturation for [Ca] = 160 mM (their Fig. 6). However, their data points are too scattered to draw definite conclusions. One paper (Mozhayeva & Naumov, 1970) does indicate a substantial Ca association constant of $K = 5.0\ \text{M}^{-1}$, with $\sigma_0 \approx -e/600\ \text{Å}^2$ for the potassium channel of frog Ranvier node.

There is one final aspect to the superposition of the curve pairs in Fig. 6*B*: if there were two charged groups on the surface – one capable and the other incapable of binding calcium – then one would not expect a simultaneous solution of Eqs. (4) and (5). The charge densities on the left side of the Equations would then represent two different quantities with σ of Eq. (4) equal to the total residual charge after binding and screening, and the σ of Eq. (5) equal to the fraction of the charge σ_0, which is capable of being neutralized by binding, and which is unbound. If these were in fact two different groups, a simultaneous solution would be unlikely and would probably require the introduction of an additional relationship. The existence of a simultaneous solution is therefore

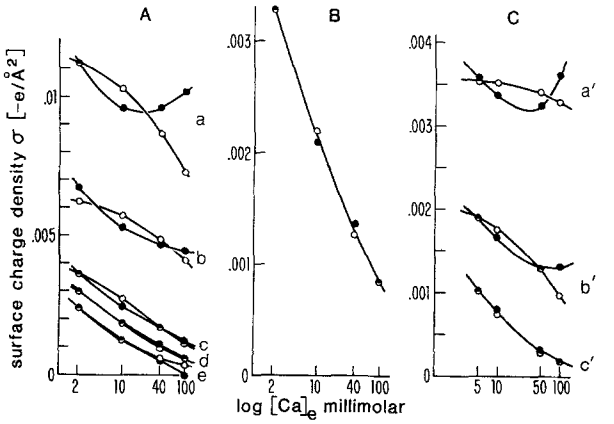

parameters for panel A

fit	σ_0	K	ψ_{ASW}
a	-1/82	0.1M^{-1}	-58mV
	-1/115	0.15	-48
b	-1/148	0.5	-38
	-1/185	2.2	-28
c	-1/194	14.0	-18
d	-1/153	60.0	-13
e	-1/87	300.0	-8

B { σ_0 = -e/182 Å^2; K = 30.0 (Moles)$^{-1}$; ψ_{ASW} = -15mV }

parameters for panel C

fit	σ_0	K	ψ_{ASW}
a'	-1/282	0.1	-29.5
b'	-1/465	5.0	-14.5
c'	-1/386	120.0	-5.7

Fig. 6. Fits of the measured relative external surface potentials for the [Ca] series to the Grahame Equation (4) (•) and the "calcium binding" Eq. (5) (o). The procedure was to assume a set of Ψ_s and values of K and σ_0 and to compute the set of four surface charge densities σ, from each equation separately. For a given set of Ψ_s [represented by $\Psi_{ASW} \equiv \Psi([\text{Ca}] = 10) + 4$ mV] the best combination of K and σ_0 was determined for Eq. (5) and compared with Eq. (4). *A*: Shows the increasing agreement as K is increased from $0.1\ \text{M}^{-1}$ to $30\ \text{M}^{-1}$ while the absolute surface potential Ψ_{ASW} decreases in magnitude from -58 to -15 mV. *B*: Expanded ordinate for the best fit from *A*. *C*: Similar to *A* with our calculations on the data of Begenisich (1975, Table III) for the *Myxicola* giant axon

consistent with the idea that a single type of charged group which is capable of binding calcium, is responsible for the surface charge phenomena studied herein.

Axoplasmic Surface Charge and Channel Gating. At the internal membrane surface, published data indicate that surface charge in a position to influence the electric field for the gating voltage sensor is small compared to the external surface. In the early years following the introduction of internal perfusion, Narahashi (1963), Moore, Narahashi and Ulbricht (1964) and Baker, Hodgkin and Meves (1964) showed that reducing the internal ionic strength (reducing KCl) shifts the threshold voltage towards zero for activating and inactivating the sodium system to generate action potentials. Direct measurements made by varying the internal ionic strength indicated a surface charge density $\sigma \approx -e/700\ \text{Å}^2$ near the sodium channels (Chandler et al., 1965). Subsequently, Rojas and Atwater (1968) estimated $\sigma \approx -e/1600\ \text{Å}^2$ on the

internal surface near the K channels. This is a very small value. Our measurements also indicate the virtual absence of surface charge on the internal membrane surface that would be in a position to influence potassium channel gating.

Surface Charge, Potentials and the Ionic Driving Force

The surface potentials near the channel pore openings were determined from the properties of the driving force, $A(E)$, defined as the measured slope of the current I_K, plotted against the instantaneous conductance g_K. A is independent of all gating mechanisms associated with delayed rectification [*cf.* Eqs. (1), (2) and (3)], and therefore refers to the flux properties of the collection of open channels. Surface charge in a position to shift the gating curve along the voltage axis will *not* influence the behavior of $A(E)$ unless it is also sufficiently near the pore mouth to change the surface potential there.

Relative Periaxonal Surface Potentials. The relative surface potential shifts at the exterior pore opening were determined by comparing the changes of $A(E)$ when the calcium concentration is changed with those when the test potential is changed. Neither the ionic strength nor the K cencentrations were altered on either membrane side for a given comparison. Shifts with calcium were relatively small, but nonzero.

Relative Axoplasmic Surface Potentials. Changing the ionic strength was the most direct method to measure potential shifts at the *internal* surface pore mouth. In this connection it is of some interest to note that the measured behavior of A as a function of E and ionic concentrations is similar to the behavior predicted by the "constant field flux equation" for which $f(E)$ is proportional to

$$f(E) \propto E \frac{a_K^{es} - a_K^{is} \exp(eE/kT)}{1 - \exp(eE/kT)}. \quad (6)$$

The instantaneous potassium current-voltage relations have previously been shown to follow the "constant field equation" for *Myxicola* axons (Binstock & Goldman, 1971; Begenisich, 1975). E is the membrane potential, and ionic strength is reflected in the activity coefficients of the potassium ion activities at the external pore mouth, a_K^{es} and internal pore mouth, a_K^{is}. From Eq. (6) it follows that when E is 'large' and positive ($\geqq +30$ mV) the term containing a_K^{is} in the numerator dominates the term a_K^{es} for all combinations of experimental K-concentrations used. Under these conditions the ratio $f/(df/dE) \equiv A(E)$ becomes independent of potassium activities, and depends only on the value of E. This is reflected in the constancy of the slope in Fig. 5 (upper panel).

For the smaller E ($= -20$ to $+5$ mV) the two terms of Eq. (6) are no longer sufficiently dissimilar to allow one of them to be neglected. In this case, the ratio $f/(\partial f/\partial E)$ depends on the potassium activities in addition to E, which predicts definitive changes in the slope A as a function of the K activities. The experimental A does indeed change as predicted (Fig. 5, lower panel).

Absolute Surface Potentials. Since an expression for $f(E)$ is at hand, the absolute surface potentials at the external pore mouth can be determined. The absence of potential variation with changes of internal ionic strength implies that the surface charge density is zero at that location and that the surface potential is equal to the bulk internal potential in all cases. Therefore, the *differences* between the voltage-clamp test potentials and the actual membrane potentials at the pore equal the *absolute external surface potentials*. These were found to be $\Psi_{es} = -5 \pm 2$ mV for 2 mM Ca, and -1 ± 2 mV for 100 mM Ca, or about -3 mV in normal sea water.

Location of Surface Charge

The small surface potentials at the pore mouth are in agreement with the findings of Begenisich (1975) for the external pore opening of the *Myxicola* K channel. Although the experimental errors of the absolute surface potentials determined above do overlap, the data do indicate some shift of the driving force $A(E)$ with changes of calcium concentration. However, this can be explained even with no charge at the pore mouth. Negatively charged calcium binding sites that influence the voltage sensor may be sufficiently near to influence the surface potential. The fraction of the voltage sensor surface potential that is present at the pore mouth is approximately

$$(-5 \text{ mV})/(-29 \text{ mV}) = e^{-1.8} \quad (7)$$

which corresponds to a separation of ~ 1.8 Debye lengths. This is equivalent to ~ 8 Å in sea water solutions (dielectric constant $\varepsilon/\varepsilon_o \approx 80$). Since the Debye length may be greater for the medium of the membrane, 8 Å is a lower limit on the separation between the voltage sensor for the gate and the channel pore.

To follow this line of reasoning one step further, it is possible that the surface charges that influence the voltage sensor are *not* located on the channel molecule at all, but instead are on the neighboring lipid. In support of this possibility we note that the association constant of calcium with phosphatidylserine [$\cong 10\ M^{-1}$ (McLaughlin et al., 1981)], the major negatively charged lipid in the squid axon membrane, is similar to the value reported here for the squid axon ($30\ M^{-1}$). The voltage sensor itself may nonetheless be well within the channel protein. A fraction of the surface potential of the lipid may then be influencing the voltage sensor. If this is the case then the potassium channel is a remarkably neutral molecule so far as electrical surface charge is concerned. However, surface charge on some part of the external face of the molecule cannot be ruled out.

Note added in Proof

Figures 4 and 5, $\alpha = A$.

References

Adelman, W.J. 1979. Tests of a simple method for continuously monitoring membrane slope conductance during voltage clamp. *Biophys. J.* **25**:14a

Baker, P.F., Hodgkin, A.L., Meves, H. 1964. The effect of diluting the internal solution on the electrical properties of a perfused giant axon. *J. Physiol. (London)* **170**:541–560

Begenisich, T. 1975. Magnitude and location of surface charges on *Myxicola* giant axons. *J. Gen. Physiol.* **66**:47–65

Binstock, L., Adelman, W.J., Senft, J.P., Lecar, H. 1975. Determination of the resistance in series with the membrane of giant axons. *J. Membrane Biol.* **21**:25–47

Binstock, L., Goldman, L. 1971. Rectification of instantaneous potassium current-voltage relations in *Myxicola* giant axons. *J. Physiol. (London)* **217**:517–531

Chandler, W.K., Hodgkin, A.L., Meves, H. 1965. The effect of changing the internal solution on sodium inactivation and related phenomena in giant axons. *J. Physiol. (London)* **180**:821–836

Conti, F., Neher, E. 1980. Single channel recordings of K^+ currents in squid axons. *Nature (London)* **285**:140–143

Eisenberg, M., Gresalfi, T., Riccio, T., McLaughlin, S. 1979. Adsorption of monovalent cations to bilayer membranes containing negative phospholipids. *Biochemistry* **18**:5213–5223

Fohlmeister, J.F., Adelman, W.J. 1981. Gating kinetics of stochastic single K-channels. *In*: The Biophysical Approach to Excitable Systems. D.E. Goldman, editor. p. 123. Plenum Press, New York

Fohlmeister, J.F., Adelman, W.J. 1982. Anomalous potassium channel gating rates as functions of calcium and potassium ion concentrations. *Biophys. J.* **37**:427–431

Frankenhaeuser, B., Hodgkin, A.L. 1957. The action of calcium on the electrical properties of squid axons. *J. Physiol. (London)* **137**:218–244

French, R.J., Wells, J.B. 1977. Sodium ions as blocking agents and charge carriers in the potassium channel of the squid giant axon. *J. Gen. Physiol.* **70**:707–724

Gilbert, D.L., Ehrenstein, G. 1969. Effect of divalent cations on potassium conductance of squid axons: Determination of surface charge. *Biophys. J.* **9**:447–463

Grahame, D.C. 1947. The electrical double layer and the theory of electrocapillarity. *Chem. Rev.* **41**:441–501

Henderson, R., Ritchie, J.M., Strichartz, G.R. 1973. The binding of labelled saxitoxin to the sodium channels in nerve membranes. *J. Physiol. (London)* **235**:783–804

Hille, B., Schwarz, W. 1978. Potassium channels as multi-ion single file pores. *J. Gen. Physiol.* **72**:409–442

Hodgkin, A.L., Keynes, R.D. 1955. The potassium permeability of a giant nerve fiber. *J. Physiol. (London)* **128**:61–88

Jakobsson, E. 1978. A fully coupled transient excited state model for the sodium channel. I: Conductance in the voltage clamped case. *J. Math. Biol.* **5**:221–242

McLaughlin, S., Mulrine, N., Gresalfi, T., Vaio, G., McLaughlin, A. 1981. Adsorption of divalent cations to bilayer membranes containing phosphatidylserine. *J. Gen. Physiol.* **77**:445–473

McLaughlin, S.G.A., Szabo, G., Eisenman, G. 1971. Divalent ions and the surface potential of charged phospholipid membranes. *J. Gen. Physiol.* **58**:667–687

Moore, J.W., Cox, E.B. 1976. A kinetic model for the sodium conductance system in squid axons. *Biophys. J.* **16**:171

Moore, J.W., Narahashi, T., Ulbricht, W. 1964. Sodium conductance shift in an axon internally perfused with a sucrose and low potassium solution. *J. Physiol. (London)* **172**:163–173

Mozhayeva, G.N., Naumov, A.P. 1970. Effect of surface charge on the steady state potassium conductance of nodal membrane. *Nature (London)* **228**:164–165

Narahashi, T. 1963. Dependence of resting and action potentials on internal potassium in perfused squid giant axons. *J. Physiol. (London)* **169**:91–115

Rojas, E., Atwater, I. 1968. An experimental approach to determine membrane charges in squid giant axons. *J. Gen. Physiol.* **51**:131s

Schauf, C.L. 1976. Comparison of two-pulse sodium inactivation with reactivation in *Myxicola* giant axons. *Biophys. J.* **16**:245–248

Sigworth, F.J., Neher, E. 1980. Single Na^+ channel currents observed in cultured rat muscle cells. *Nature (London)* **287**:447–449

Received 4 January 1982; revised 8 March 1982;
revised again 4 May 1982